



## Theory-guided efficient strategy to maximize speed and resolution in rapid gradient LC–MS/MS bioanalysis

Jian Wang<sup>a,\*</sup>, Jingpin Jia<sup>b</sup>, Anne Aubry<sup>a</sup>, Mark Arnold<sup>a</sup>, Mohammed Jemal<sup>c,\*\*</sup>

<sup>a</sup> Bristol-Myers Squibb, Research & Development, Analytical and Bioanalytical Development, Princeton, NJ 08543, United States

<sup>b</sup> New Brunswick, NJ 08903, United States

<sup>c</sup> Bioanalytical and Discovery Analytical Sciences, Princeton, NJ 08543, United States

### ARTICLE INFO

#### Article history:

Received 4 January 2011

Accepted 14 May 2011

Available online 26 May 2011

#### Keywords:

LC–MS/MS bioanalysis

Rapid gradient elution

Flow rate

Resolution

Peak capacity

### ABSTRACT

Reversed-phase gradient LC–MS/MS bioanalytical methods of 5–100% organic solvent in a 1–3 min gradient time are common in today's bioanalytical laboratory. The goal of this work was to develop a theory-guided systematic strategy for maximizing resolution and speed in rapid gradient LC–MS/MS bioanalysis. We studied the effect of gradient time ( $t_G$ ), initial and final eluent strength (%  $B$  = % organic), and flow rate ( $F$ ) on the separation of multiple critical pairs ( $R_s$ ) and peak capacity ( $n_c$ ) in a gradient elution of a mixture of five structurally related compounds. By optimizing the gradient time  $t_G$ , the initial and final percentages of the organic component of the mobile phase, comparable resolution and peak capacity could be achieved in a shorter run time. More importantly, we demonstrated that higher flow rates improved resolution, peak capacity and reduced run time in rapid gradient separations on a 5  $\mu\text{m}$  particle column. A straightforward mathematical explanation of the phenomenon was provided applying basic resolution equations in gradient elution theory. A systematic approach to execute a rapid gradient LC–MS/MS bioanalytical method to shorten run time and improve resolution is proposed, taking into consideration not only the analytes of interest but also potential matrix effects from the dosing vehicle and biological matrix.

© 2011 Elsevier B.V. All rights reserved.

### 1. Introduction

Rapid gradient LC–MS/MS methods with short run times have been widely used in analyzing samples from pharmacokinetics (PK) studies in drug discovery and development. In bioanalytical reversed-phase LC methods, linear gradient elution on short 5-cm columns in less than 3 min is quite common [1–8]. Bioanalysts tend to apply a generic approach of starting the gradient program with a mobile phase of low organic content and ending with a mobile phase of high organic content without due consideration as to where the analytes elute vis-à-vis the column dead volume time and the end of the gradient time.

The effect of gradient parameters and the optimization scheme, in the rapid gradient LC–MS/MS setting, were studied using a test

mixture of four analytes and one internal standard, which represents a moderately complex example of bioanalytical method development. The central theme of the work presented in this paper deals with the efficient use of gradient elution to achieve the required separation following the selection of the column, and mobile phases A and B. The chromatographic theory of the linear-solvent-strength (LSS) model [9–11] lays the basis for the optimization of gradient elution to achieve the best possible resolution per unit time.

Neue et al. related peak capacity to gradient elution parameters [2,12–15]. They studied the effect of gradient time, flow rate, temperature, column length and particle size on the maximum possible peak capacity in a gradient elution where gradient time  $t_G$  instead of the time window between the first and last actual peaks ( $t_{R,f} - t_{R,1}$ ) was used. They did point out that in general, higher resolution is achieved at high flow rates, especially for rapid gradients from 0 to 100% organic, but no explanation of this phenomenon was provided. Wang et al. optimized peak capacity in gradient elution on a 2.1  $\times$  50 mm, 3.5  $\mu\text{m}$  column for peptide separation [16]. They studied effect of gradient time, flow rate, temperature, and final eluent strength on peak capacity. Their goal was to achieve the maximum separation for the tryptic peptides of a protein within the maximum acceptable run time (up to 2 h, in their laboratory), Wang et al. also concluded that there were strong interactions between individual

\* Corresponding author at: Analytical and Bioanalytical Development, Bristol-Myers Squibb, Research & Development, Route 206 and Province Line Road, Princeton, NJ 08543, United States. Tel.: +1 609 252 3856, fax: +1 609 252 6171.

\*\* Corresponding author at: Bioanalytical and Discovery Analytical Sciences, Bristol-Myers Squibb, Research and Development, Route 206 and Province Line Road, Princeton, NJ 08543, United States. Tel.: +1 609 252 3572, fax: +1 609 252 3315.

E-mail addresses: [jian.wang@bms.com](mailto:jian.wang@bms.com) (J. Wang), [mohammed.jemal@bms.com](mailto:mohammed.jemal@bms.com) (M. Jemal).

gradient elution variables (e.g., gradient time and flow rate) which make the optimization quite complicated. In a more recent publication, Petersson et al. [17] conducted a thorough investigation of the effect of flow rate, gradient slope and temperature on peak capacity using the same equations as Neue et al. [2,12–15]. They demonstrated that the maximum peak capacities were achieved at maximum gradient times and flow rates when performing gradient elution on sub-2  $\mu\text{m}$  particle columns at temperature above 45 °C. This unexpected observation was convincingly explained through application of the gradient theory.

Even though peak capacity is a useful concept in describing the resolving power of a method for complex mixtures, other parameters such as resolution are often more meaningful to describe an actual separation. In this paper, we present the effect of gradient parameters – gradient time ( $t_G$ ), initial and final % B and flow rate ( $F$ ) – on the resolution ( $R_s$ ) of critical pairs in a mixture of analytes from a current BMS development project. Conditions typical of fast gradient LC–MS/MS bioanalytical methods with a 2.1  $\times$  50 mm column, 3  $\mu\text{m}$  or 5  $\mu\text{m}$  particles and a  $t_G$  of 1–3 min were used to separate the 5 compounds. The effect of  $F$  on  $R_s$  in a rapid gradient bioanalytical method was systematically examined experimentally and explained theoretically using equations of the LSS model. The work presented herein also deals with the misconception that the optimal flow rate determined under isocratic elution will also be optimal under gradient elution, a point previously addressed by others [16,17]. Finally, we present a systematic approach to execute a gradient LC–MS/MS bioanalytical method to achieve shorter run time and improved resolution.

## 2. Theory

The LSS model for HPLC gradient elution was developed by Snyder et al. [9–11] and has since been applied by others in attempts to make gradient method development less empirical.

The resolution between two chromatographic peaks is defined as [10]:

$$R_s = \frac{1.18(t_2 - t_1)}{W_{1/2,1} + W_{1/2,2}} \quad (1)$$

where  $t_1$  and  $t_2$  are the retention times of the two peaks while  $W_{1/2,1}$  and  $W_{1/2,2}$  are the peak widths at half height of the two peaks.

The separation power of a gradient elution can also be measured by peak capacity  $n_c$  [12–15,17]:

$$n_c = \frac{t_G}{W} \quad (2)$$

where  $t_G$  is the gradient time and  $W$  is the average peak width.

Because in a real separation, peaks will only occupy a fraction of the gradient, other authors have suggested the following alternative equation [16]:

$$n_c = \frac{t_{R,f} - t_{R,1}}{W} \quad (3)$$

where  $t_{R,1}$  and  $t_{R,f}$  are the retention times of the first and last real peaks in the chromatogram,  $W$  is the average peak width.

Resolution  $R_s$ , in an isocratic elution, can also be expressed as [10]:

$$R_s = \left(\frac{1}{4}\right) N^{1/2} (\alpha - 1) \left[\frac{k}{1+k}\right] \quad (4)$$

where  $N$  is the column plate number which can be calculated by  $N = 5.54(t_R/W_{1/2})^2$  in isocratic elution.  $k$  is the (average) retention factor of the two adjacent peaks, and  $\alpha$  is the separation factor ( $\alpha = k_2/k_1$ , where  $k_1$  and  $k_2$  are values of  $k$  for the adjacent peaks 1 and 2).

The retention factor  $k$  in isocratic elution or  $k_g$  in gradient elution [12] is defined as:

$$k(\text{or } k_g) = \frac{t_R - t_0}{t_0} \quad (5)$$

where  $t_R$  is the peak retention time and  $t_0$  is the column dead volume time.

In gradient elution, Snyder used the concept of the effective or average retention factor,  $k^*$ , which is defined by the following equation for small molecules [9–11]:

$$k^* = \frac{20t_G F}{V_m(\Delta\%B)} \quad (6)$$

where  $t_G$  is the gradient time (min),  $F$  is flow rate (mL/min),  $V_m$  is the column dead volume,  $\Delta\%B$  is the difference between the initial and final % B.

Combining equations derived by Snyder et al. [9–11] and Neue et al. [12] the  $R_s$  in gradient elution can be expressed as:

$$R_s = \left(\frac{1}{4}\right) N^{1/2} \ln(a) \left[\frac{k^*}{2+k^*}\right] \quad (7)$$

Eq. (7) nicely links the effective retention factor  $k^*$  to resolution in gradient elution in the same way that the retention factor  $k$  is linked to resolution in isocratic elution, which makes it useful in designing a gradient elution. It should be noted that the  $\alpha$  term in the  $R_s$  equation has taken different forms in the literature –  $(\alpha - 1)$ ,  $(\alpha - 1)/\alpha$ , or  $\ln(\alpha)$  – but the different forms are mathematically equivalent when  $\alpha$  is close to 1, as shown by our calculations (data not shown) using the  $\alpha$  values obtained from our experiments.

## 3. Experimental

### 3.1. Chemicals and materials

The five proprietary compounds used in the experiments described herein were provided by Discovery Chemistry of Bristol-Myers Squibb Co. (Princeton, NJ). A mixture of five compounds each of 10 ng/mL in water/acetonitrile (50/50, v/v) was used in all the experiments. Deionized water (>18 M $\Omega$ ) was prepared from a Milli-Q purification system from Millipore Corporation (Millford, MA). HPLC grade acetonitrile was purchased from Burdick & Jackson (Muskegon, MI). ACS grade formic acid was purchased from EM Science (Gibbstown, NJ). Ammonium formate was purchased from J.T. Baker (Phillipsburg, NJ). Polyethylene glycol (average molecular weight = 400, PEG400) was purchased from Sigma–Aldrich (St. Louis, MO) and 0.01% PEG400 was prepared in water/acetonitrile (50/50, v/v).

### 3.2. LC–MS/MS conditions

The mass spectrometer used was a Sciex API4000 triple quadrupole instrument from Applied Biosystems/MDS Sciex (Concord, Ontario, Canada). The HPLC system used was Shimadzu LC-10ADvp pumps (Columbia, MD) in an Aria TLX2 configuration from Thermo Fisher Scientific–Cohesive Technologies (Franklin, MA). There was a 0.167-min adjustment for  $t_R$  related calculations due to 10 s delay in mass spectrometer acquisition after injection due to Aria software. The autosampler was a CTC HTS PAL from LEAP Technologies (Carrboro, NC). The injection volume was 10  $\mu\text{L}$ . The API4000 mass spectrometer was operated in Turbo Ion-Spray mode and the MS/MS detection of each compound was performed in the multiple reaction monitoring (MRM) mode. Each mass spectrometer parameter was kept constant in all the experiments conducted, e.g., CUR=30, GS1=50, GS=50, CAD=6, IS=4500 V, and EP=10. All compound related

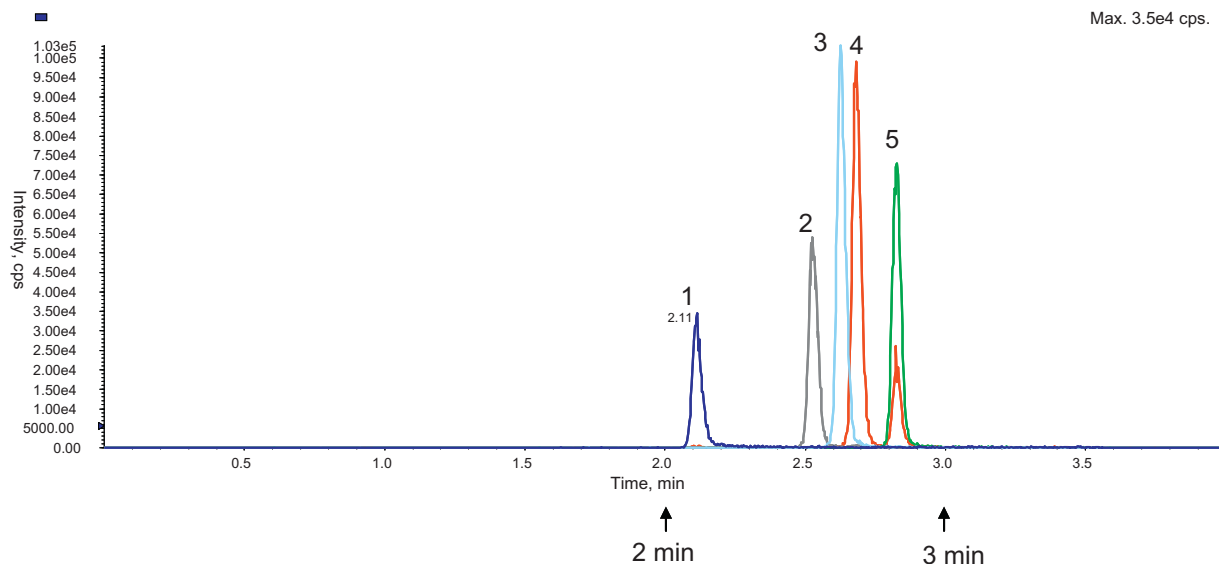


**Fig. 1.** A mixture of compounds of 1–5 on Luna C18 (2),  $2 \times 50$  mm,  $3 \mu\text{m}$  with mobile phase A of 10 mM ammonium formate/0.1% formic acid in water and mobile phase B of 0.1% formic acid in acetonitrile. The gradient was 5–100% B in 3 min with a flow rate of  $400 \mu\text{L}/\text{min}$ . ( $k^* = 2.5$ ). Compound 5 gives response in the MRM channel monitored for compound 4 (red), in addition to its own MRM channel. (For interpretation of the references to color in this figure legend, the reader is referred to the web version of the article.)

parameters – DP, CE, CXP – were kept constant and the dwell time was 30 ms for each compound. The MRM for each compound is not listed here as the information is not relevant to the theme of this paper. A syringe pump from Harvard Apparatus (Holliston, MA) was used in the post-column infusion experiments.

Gradient chromatographic experiments were carried on either a  $3 \mu\text{m}$  or  $5 \mu\text{m}$  Luna C18 (2),  $2 \times 50$  mm column (Phenomenex, Torrance, CA, USA). LC Mobile phase A was 10 mM ammonium formate/0.1% formic acid in water and mobile phase B was 0.1% formic acid in acetonitrile. The chromatographic conditions in the experiments conducted were as follows: first, the gradient time,  $t_G$ , was varied from 1 to 12 min while the other gradient variables were kept constant, e.g., flow rate ( $F$ ) =  $400 \mu\text{L}/\text{min}$ , initial % B = 5, and final % B = 100. Second, the initial % B was varied from 5 to 80 at 5, 20, 30, 40, 50, 60, 70, 80 while the other gradient variables were kept constant, e.g., flow rate  $F$  =  $400 \mu\text{L}/\text{min}$ , final % B = 100, and  $t_G$  = 3 min. Third, the final % B was varied from 100 to 50 at 100, 90, 80, 70, 60, 50 while the other gradient variables were kept constant, e.g., flow rate  $F$  =  $400 \mu\text{L}/\text{min}$ , initial % B = 40, and  $t_G$  = 3 min. Fourth, the flow rate  $F$  was varied from 0.1 to 1 mL/min at 0.1, 0.2, 0.3, 0.4, 0.5, 0.6, 0.8, 1.0 mL/min while the other gradient variables were kept constant, e.g., initial % B = 40, final % B = 100,  $t_G$  = 3 min. In all experiments, the chromatographic run was continued for at least 2 min beyond the gradient time.

Isocratic experiments were conducted to calculate the column efficiency at various flow rates ( $F$  = 0.1, 0.2, 0.3, 0.4, 0.5, 0.6, 0.8, 1.0 mL/min) at 58% B. A  $5 \mu\text{m}$  Luna C18 (2),  $2 \times 50$  mm column was used in the experiments when the flow rate was varied while a  $3 \mu\text{m}$  Luna C18 (2),  $2 \times 50$  mm column was used for the rest of the experiments. The chromatographic conditions in the experiments are also detailed in Section 4 and described in the figure captions. All experiments were conducted in at least triplicates and the average from at least three measurements is presented in the data shown.

Biologic matrix effect was tested with selected gradient elution methods by conducting post column infusion of the analyte solution while injecting rat plasma extract, obtained via acetonitrile protein precipitation and diluted PEG400 solution [18].

## 4. Results and discussion

### 4.1. Typical rapid gradient elution in LC–MS/MS bioanalysis

In a common rapid gradient elution method depicted in Fig. 1, 5–100% organic mobile phase B in 3 min with a flow rate of  $400 \mu\text{L}/\text{min}$ , a chromatogram obtained with a sample containing four analytes plus an analogue internal standard is shown. Compound 1 is a pro-drug of the active compound 4; compounds 2 and 5 are the metabolites of the parent compound 4 and compound 3 is the internal standard. This mixture of compounds represents a typical drug mixture sample from biological matrices in pharmacokinetic studies and contains chromatography separation challenges commonly seen in rapid gradient LC–MS/MS bioanalysis: compound 5 gives a response in the SRM channel of the parent compound 4 as can be seen by the red trace at the retention time of compound 5; compounds 1, 4 and 5 can undergo in-source conversion and interfere with compound 2. Therefore, chromatographic separation was required between compounds 4 and 5, as well as between compound 2 and compounds 1, 4 and 5. The chromatogram in Fig. 1 achieves acceptable resolution between interfering peaks but improved resolutions are desirable. One additional observation from this chromatogram is that all five compounds elute after 2 min leaving the first 2 min or two-thirds of the gradient time, devoid of any peak, which is a waste of instrument time. The ultimate goal of high throughput bioanalysis is high speed analysis with high quality data.

As presented in Eq. (7), the resolution of a gradient elution is governed by the column efficiency  $N$  term, selectivity  $\alpha$  term, and the retention  $k^*$  term. Plate number  $N$  is determined by the column length, particle size, and flow rate. It should be noted that  $N$  is also a function of the retention factor and is also analyte dependent [17,18]. Selectivity  $\alpha$  is largely controlled by column stationary phase and mobile phase. As shown in Eq. (6),  $k^*$  is affected by gradient time ( $t_G$ ), flow rate ( $F$ ), column dead volume ( $V_m$ ), and the difference between the initial and final % mobile phase B ( $\Delta\% B$ ). Screening columns and mobile phases is one of the options to achieve improved chromatography resolution. Meanwhile, for a fixed column and mobile phases the gradient variables defined in Eq. (6) determine the resolution. The compound mixture depicted

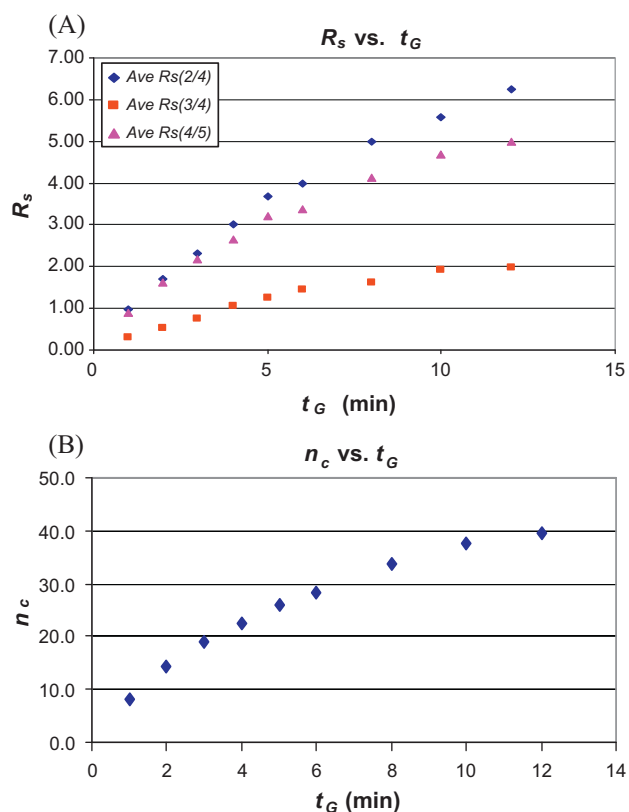


**Fig. 2.** Effect of gradient time ( $t_G$ ) on (A)  $R_s$  between peaks 2/4, 3/4, and 4/5, and on (B) peak capacity ( $n_c$ ). Other variables are  $F=400 \mu\text{L}/\text{min}$ ,  $\Delta\% B=5\text{--}100$  using the column and mobile phases A and B described in Fig. 1.

in Fig. 1 were used to demonstrate the effect of these gradient elution parameters on the resolution ( $R_s$ ) in rapid gradient elution, calculated using Eq. (1), of three critical pairs: 2/4, 3/4, and 4/5. The effect on the peak capacity ( $n_c$ ), calculated using Eq. (3), was also evaluated. It should be noted that in this equation  $W_{1/2}$  (peak width at half height) was used instead of  $W$  (peak width at baseline) for ease of determination by the mass spectrometer software.

#### 4.2. The effect of gradient time ( $t_G$ )

Although gradient time of  $t_G=1\text{--}3$  min is most common in a rapid gradient LC–MS/MS bioanalytical method, for illustration purpose, the effect of changing the gradient time ( $t_G$ ), with the other gradient elution variables kept constant, on the  $R_s$  of three critical pairs and on the  $n_c$  was evaluated at  $t_G$  up to 12 min, which was beyond what bioanalysts would consider a rapid gradient. Results are shown in Fig. 2. Longer gradient times generate higher resolution and peak capacity which is consistent with reports in the literature [13–17]. As summarized in Table 1, the retention time  $t_R$  and peak widths of the first and last peaks also increase when  $t_G$  increases.  $k^*$  increased from 0.84 at  $t_G=1$  min to 10.1 at  $t_G=12$  min. At  $t_G=1$  min, all five compounds eluted after the gradient completed. When  $t_G$  and  $k^*$  increase, the first and last peaks elute at relatively lower %B. Increasing  $t_G$  to improve  $R_s$  and  $n_c$  is not the best option for bioanalysis, where short run times and fast turnaround of sample analysis is essential. The shortest  $t_G$  gaining sufficient  $R_s$  is preferred. In this particular example,  $t_G$  of 4–6 min with the corresponding  $k^*$  of 3.4–5.0 provide adequate resolution and a good balance between performance and run time. As an example, the following resolution values are obtained at  $t_G$  of 5 min and  $k^*$  of 4:  $R_s(2/4)=3.68$ ,  $R_s(3/4)=1.27$ , and  $R_s(4/5)=3.20$ .

**Table 1**

The effect of gradient time on the first and last peak retention times and other parameters associated with the two peaks. The resolution and peak capacity results obtained for the same experiment are shown in Fig. 2.

$t_G$ (min)	$k^*$	$t_R$ first peak (min)	$t_R$ last peak (min)	$W_{1/2}$ first peak (min)	$W_{1/2}$ final peak (min)	% B final peak	% B final peak	$W_{1/2}$ final peak (min)	$t_1/t_0$	$\Delta t$ final – first (min)
1	0.84	1.21	1.51	0.0361	0.0381	100 <sup>f</sup>	100 <sup>f</sup>	0.0381	4.8	0.30
2	1.68	1.76	2.29	0.0401	0.0352	89	100 <sup>f</sup>	0.0352	7.1	0.53
3	2.52	2.26	3.00	0.0425	0.0375	77	100 <sup>f</sup>	0.0375	9.0	0.74
4	3.36	2.73	3.66	0.0444	0.0399	70	92	0.0399	10.9	0.93
5	4.20	3.18	4.29	0.0472	0.0422	65	87	0.0422	12.7	1.12
6	5.0	3.61	4.90	0.0490	0.0452	62	83	0.0452	14.4	1.29
8	6.72	4.44	6.07	0.0526	0.0475	58	77	0.0475	17.8	1.63
10	8.40	5.25	7.20	0.0534	0.0513	55	73	0.0513	21.0	1.95
12	10.1	6.04	8.28	0.0596	0.0566	53	71	0.0566	24.2	2.24

1.  $k^*$  as calculated using Eq. (6).

2.  $t_R$  (retention time) of the first and last peaks as measured.

3. % B for the first and last peaks as calculated using the respective retention times and the elution gradient program.

4.  $W_{1/2}$  (peak width at half height) as measured.

5.  $t_1/t_0$  as calculated using the retention time of the first peak ( $t_1$ ) and the column dead time ( $t_0$ ).  $t_0$  is calculated by using the equation  $t_0=0.5Ld^2/F$ , where  $L$  is the column length in cm,  $d$  is the column diameter in cm, and  $F$  is the flow rate in mL/min.

6.  $\Delta t$  (retention time window) is the difference between the first and last peak retention times.

<sup>f</sup> At 100% B plateau.

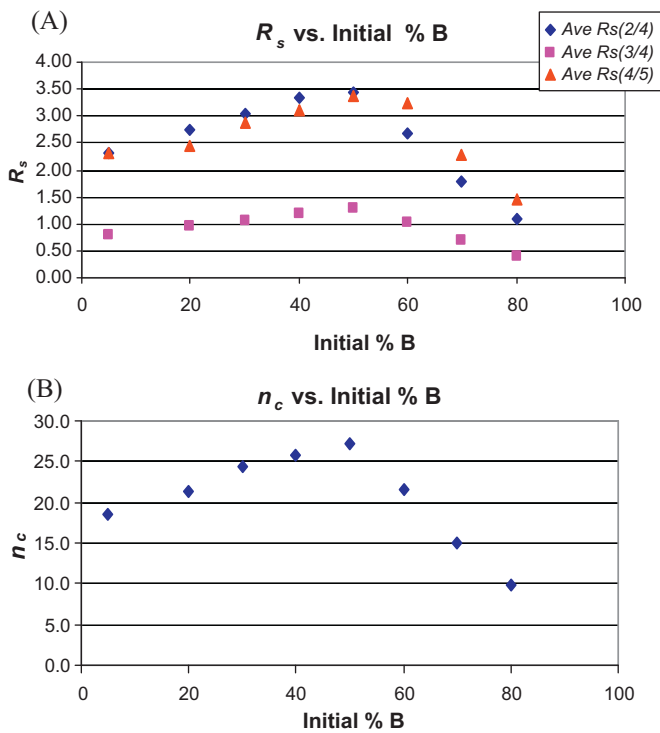


**Fig. 3.** Effect of initial % B on (A)  $R_s$  between peaks 2/4, 3/4, and 4/5, and on (B) peak capacity ( $n_c$ ). Other parameters:  $F=400 \mu\text{L}/\text{min}$ ,  $t_G=3 \text{ min}$ , final % B = 100 using the column and mobile phases A and B described in Fig. 1.

4.3. The effect of initial and final eluent strength (% B)

The effect of changing the initial % B, with the other gradient elution variables kept constant, is shown in Fig. 3. The  $R_s$  of all the three critical pairs and the  $n_c$  reach a maximum at initial % B = 50. Retention time  $t_R$  of all five peaks become shorter when the initial % B increases. The difference in the average peak width between 5 and 50% B is negligible and a slight increase is observed when the initial % B is above 60. When the initial % B is beyond a certain high value, e.g., 60, the high-organic shallow gradient elution results in a blast elution of the early eluting components with reduced resolution [10].  $k^*$  increased from 2.5 at initial % B value of 5–12 at initial % B value of 80 as calculated by Eq. (6). Increasing initial % B has the potential of reducing run time and thus it is a more appealing option to improve  $R_s$  and  $n_c$  in a bioanalytical method. The peak widths and the retention times of the first and last peaks as a function of initial % B are summarized in Table 2.

The effect of the final % B was also evaluated at 100, 90, 80, 70, 60, and 50 with the initial % B set at 40 (data not shown). The resolution  $R_s$  of all the three critical pairs increase when final % B is decreased from 100 to 50%, with some of the late eluting peaks eluting beyond the gradient time  $t_G$  when the final % B is below ~75. The average peak width, the retention times of all peaks, and the retention time window increased with a decrease in the final % B. The results indicate that the optimum final % B needs to be determined experimentally for a particular mixture of compounds.

4.4. The effect of flow rate (F)

Flow rates of 0.1, 0.2, 0.3, 0.4, 0.5, 0.6, 0.8, and 1.0 mL/min were evaluated on a  $2 \times 50 \text{ mm}$ ,  $5 \mu\text{m}$  column and the resulting chromatograms are shown in Fig. 4 while the  $R_s$  and  $n_c$  results are shown in Fig. 5. When the flow rate increases, the compounds elute with shorter retention times and within a narrower retention time window, the % B at the elution of the last peak decreases, and the  $t_0$

**Table 2** The effect of initial % B on the first and last peak retention times and other parameters associated with the two peaks. The resolution and peak capacity results obtained for the same experiment are shown in Fig. 3.

Initial % B	$k^*$	$t_G$ first peak (min)	$t_R$ first peak (min)	$W_{1/2}$ first peak (min)	% B first peak	$t_R$ final peak (min)	$W_{1/2}$ final peak (min)	% B final peak	$W_{1/2}$ final peak (min)	$t_1/t_0$	$\Delta t$ final – first (min)
5	2.5	2.28	77	0.0417	100 <sup>†</sup>	2.99	0.0374	100 <sup>†</sup>	0.0374	9.1	0.72
20	3.0	1.97	73	0.0417	95	2.82	0.0390	95	0.0390	7.9	0.85
30	3.4	1.68	69	0.0427	92	2.64	0.0380	92	0.0380	6.7	0.96
40	4.0	1.31	66	0.0445	88	2.40	0.0407	88	0.0407	5.2	1.09
50	5.0	0.89	65	0.0489	84	2.06	0.0425	84	0.0425	3.6	1.16
60	6.0	0.63	68	0.0524	68	1.64	0.0433	82	0.0433	2.5	1.01
70	8.0	0.50	75	0.0478	75	1.21	0.0472	82	0.0472	2.0	0.71
80	12.0	0.45	83	0.0460	83	0.88	0.0438	86	0.0438	1.8	0.43

<sup>†</sup> At 100% B plateau.

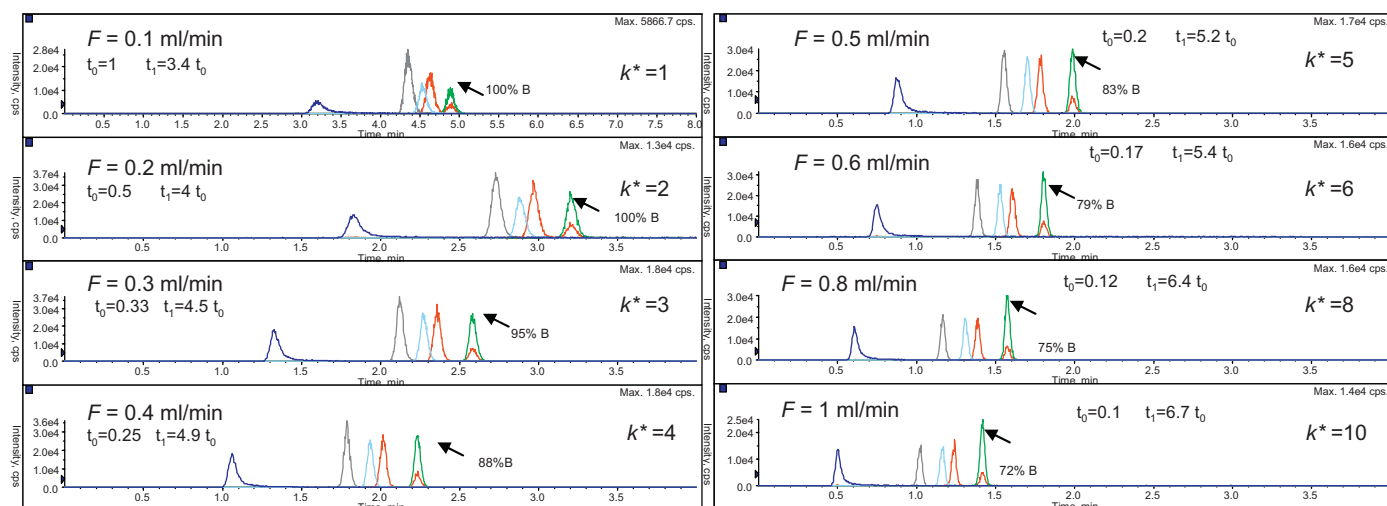


**Fig. 4.** Chromatograms of a mixture of five compounds 1–5 at different flow rates. Other parameters:  $t_C = 3$  min, initial %  $B = 40$  and final %  $B = 100$ . Column: Luna C18 (2),  $2 \times 50$  mm,  $5 \mu\text{m}$ .

decreases while the  $t_1/t_0$  increases indicating that the first peak is better separated from the solvent front. The peak widths and the retention times of the first and last peaks and related information are summarized in Table 3. As shown in Fig. 5, higher  $R_s$  and  $n_c$  were obtained at higher flow rates. These results demonstrate that running at a higher flow rate in a rapid gradient elution mode will reduce run time and improve resolution, and peak capacity. This is in contrast with isocratic elution in which a decrease in

resolution is expected at high flow rates. This enhanced peak capacity at high-flow in (rapid) gradient elution were reported by Neue [13] and Wang et al. [16]. Petersson et al. [17] reported the similar results on sub- $2 \mu\text{m}$  particle columns and provided an excellent and convincing explanation for this unexpected phenomenon by correlating experimental and calculated results using peak capacity equations and also linked the phenomenon to the empirical van Deemter equation. Nonetheless, their calculating peak capacity using  $t_C$  (Eq. (2)) instead of  $t_{R,f} - t_{R,1}$  (Eq. (3)) in a mixture overestimated the change of peak capacity and resolving power of a method. As Wang et al. [16] appropriately pointed out, a real sample generally occupies only a fraction of the maximum possible time window  $t_C$ . Using the full gradient time  $t_C$  to calculate the peak capacity results in a hypothetical maximum peak capacity which may never be achieved in real sample analysis.

In the current work, the impact of flow rate on rapid gradient elution was probed by applying the resolution equations from Snyder (Eqs. (6) and (7)). Because our test mixture was behaving as a “regular” sample mixture per Snyder’s definition [9–11]. The resolution ( $R_s$ ) results matched well with the peak capacity and confirmed the  $R_s$  changes of individual critical pairs was consistent with the change of resolving power for the mixture under different conditions.

#### 4.4.1. Resolution increases as a function of flow rate

There is a key difference between  $k$  used in isocratic resolution Eq. (4) and  $k^*$  used in gradient resolution Eq. (7). Retention factor  $k$  in isocratic elution is independent of flow rate (Eq. (5)) but  $k^*$  in gradient elution is affected by flow rate (Eq. (6)). In an isocratic elution the optimum flow rate for resolution  $R_s$  of a method is the same as the optimum flow rate for column efficiency  $N$ . On the other hand, in gradient elution, the optimum flow rate for resolution  $R_s$  or peak capacity  $n_c$  is not necessarily the same as the optimum flow rate for column efficiency  $N$ .

In gradient elution, as can be seen from Eqs. (6) and (7), both  $N$  and  $k^*$  are affected by flow rate. Just as in isocratic mode, column efficiency  $N$  reaches a maximum at a certain flow rate determined by van Deemter curve and further increase of flow rate will decrease  $N$ . On the other hand,  $k^*$ , and hence the  $k^*/(2+k^*)$  term in Eq. (7), increases as the flow rate increases. Thus, at high flow rates, the effect of flow rate on  $N$  is opposite to that on  $k^*$ . It is reasonable to assume that selectivity  $\alpha$  changes follows the same trend as the  $k^*/(2+k^*)$  term. Putting all these factors and trends into the mathematical relations defined by Eqs. (6) and (7), it can be deduced that

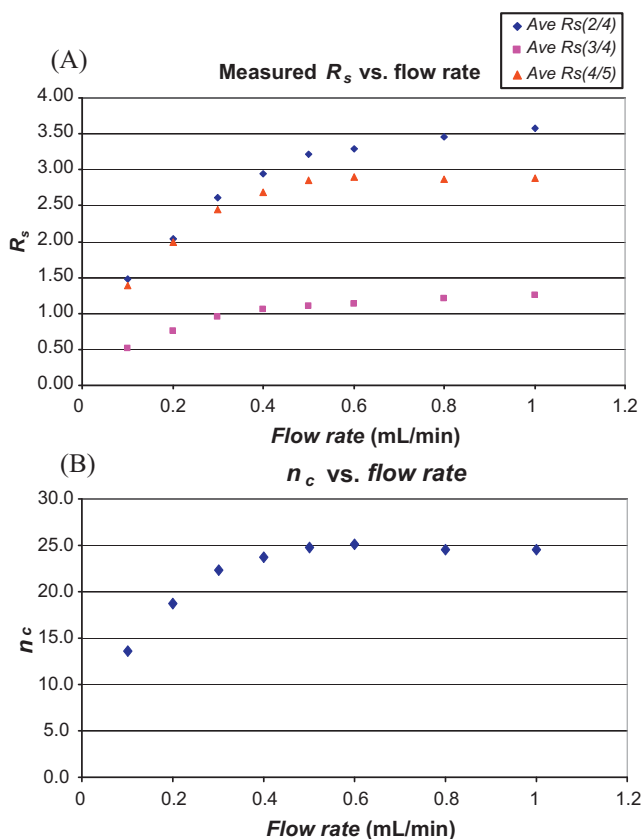


**Fig. 5.** Effect of flow rate ( $F$ ) on  $R_s$  between peaks 2/4, 3/4, and 4/5 (A), and on peak capacity ( $n_c$ ) (B). Average  $W_{1/2}$  of 5 peaks was used in  $n_c$  calculation. Other parameters:  $t_C = 3$  min, initial %  $B = 40$  and final %  $B = 100$ . Column: Luna C18 (2),  $2 \times 50$  mm,  $5 \mu\text{m}$ .

**Table 3**  
The effect of flow rate ( $F$ ) on the first and last peak retention times and other parameters associated with the two peaks. The resolution and peak capacity results obtained for the same experiment are shown in Figs. 4 and 5.

$F$ (mL/min)	$k^*$	$t_R$ first peak (min)	% $B$ first peak	$W_{1/2}$ first peak (min)	$t_G$ first peak (min)	$t_G$ final peak (min)	% $B$ final peak	$W_{1/2}$ final peak (min)	$t_1/t_0$	$\Delta t$ final – first (min)
0.1	1	3.36	100 <sup>†</sup>	0.1790	5.05	5.05	100 <sup>†</sup>	0.1097	3.4	1.69
0.2	2	2.01	80	0.0906	3.37	3.37	100 <sup>†</sup>	0.0691	4.0	1.36
0.3	3	1.49	70	0.0669	2.75	2.75	95	0.0535	4.5	1.25
0.4	4	1.22	64	0.0592	2.39	2.39	88	0.0477	4.9	1.17
0.5	5	1.04	61	0.0538	2.16	2.16	83	0.0434	5.2	1.11
0.6	6	0.92	58	0.0503	1.97	1.97	79	0.0409	5.4	1.06
0.8	8	0.77	55	0.0459	1.74	1.74	75	0.0386	6.4	0.97
1.0	10	0.67	53	0.0413	1.58	1.58	72	0.0369	6.7	0.92

<sup>†</sup> At 100%  $B$  plateau.

at high flow rates, up to 1 mL/min as shown in Fig. 5, the larger values of  $k^*$  (and possibly  $\alpha$ ) could more than make up for the decrease in  $N$ , resulting in higher  $R_s$ . Thus, in gradient elution  $R_s$  could reach the optimum at a flow rate which is significantly higher than that in isocratic elution.

High flow rate rapid gradient elution LC–MS/MS method with a 3 or 5  $\mu\text{m}$  particle column has been common in high throughput bioanalytical applications and most of those who practiced in this fashion normally acknowledged that  $R_s$  or separation was compromised for speed. Turning to smaller particle (e.g., sub-2  $\mu\text{m}$ ) column uHPLC was indentified as the (only) viable option to achieve high resolution separation at high flow rate for high speed analysis [19–22]. In various vendor brochures, presentations, and publications on sub-2  $\mu\text{m}$  particle column and uHPLC technology it is often stated that 3 and 5  $\mu\text{m}$  particle columns achieve best separation efficiency at lower flow rate, e.g.,  $\sim 100$ – $200$   $\mu\text{L}/\text{min}$  (for a 2 mm ID column), determined by van Deemter curves [19] and running at high flow rates will reduce separation/resolution power on these columns which is true in isocratic elution. Our results demonstrated that higher resolution and peak capacity in gradient LC elution are achieved at higher flow rate on a 5  $\mu\text{m}$  particle stationary phase as Petersson et al. demonstrated on 1.7  $\mu\text{m}$  particle columns [17]. It is obvious that achieving higher resolution/peak capacity at higher flow rate in a gradient method is a relatively easier task with sub-2  $\mu\text{m}$  particles than with 5  $\mu\text{m}$  particles. The optimal flow rate for column  $N$  is much higher for a sub-2  $\mu\text{m}$  particle stationary phase and the van Deemter curve stays relatively flat in the usable flow rate region 0.5–1.5 mL/min [17,19] indicating that the loss of column efficiency at higher flow rate from a sub-2  $\mu\text{m}$  particle column is much less than on a 5  $\mu\text{m}$  column which is the foundation for the current practice with sub-2  $\mu\text{m}$  particle columns for speed and resolution.

The experimental data suggest that this favorable effect of flow rates is more profound for rapid gradient elution especially those from 0 to 100%  $B$ . This can be explained using Eqs. (6) and (7). In Eq. (7), mathematically, the maximum value of the retention term  $k^*/(2+k^*)$  is close to 1.0 when  $k^*$  tends to infinity. Meanwhile,  $k^*$  as defined by Eq. (6) is affected by the combination of  $t_G$ ,  $F$ ,  $V_m$ , and  $\Delta\% B$ .

A rapid and steep gradient elution may involve a short  $t_G$  (e.g., 1–3 min) and a large  $\Delta\% B$  (e.g., 0–100%  $B$ ). With small  $t_G$  and large  $\Delta\% B$ , a large  $F$  value (high flow rate) is needed to obtain  $k^*$  large enough to bring the  $k^*/(2+k^*)$  term close to 1.0. On the other hand, in a slow gradient elution, e.g.,  $t_G = 30$  min, such as LC–UV methods developed for analysis of active pharmaceutical ingredients, the  $t_G$  in Eq. (6) is large enough so that the  $k^*/(2+k^*)$  term is close to 1.0 even at relatively low flow rates. Hence, increasing the flow rate will not have the significant effect it has when a short  $t_G$  is used. Under these circumstances, the flow rate that gives optimum resolution, obtained using Eq. (7), is close to the flow rate that gives the highest  $N$ . The same is true for a shallow gradient, due to the effect of the smaller  $\Delta\% B$  term on  $k^*$  in Eq. (6).

The interplay of the gradient elution parameters described above is shown graphically in the theoretical plots of  $k^*/(2+k^*)$  vs. flow rate shown in Fig. 6, with  $F$  ranging from 0.1 to 2 mL/min,  $t_G = 1, 2, 3, 6, 12, 20$  and 30 min, and with  $\Delta\% B = 100$  and  $\Delta\% B = 40$ , respectively on a  $2 \times 50$  mm column. With  $\Delta\% B = 100$  (Fig. 6A), it can be seen that at short  $t_G$  of 1, 2 or 3 min (blue, pink and yellow lines, respectively), the  $k^*/(2+k^*)$  term, significantly small at lower flow rates, continues to increase with flow rate up to the highest flow rate ( $F = 2$  mL/min). In contrast, at higher values of  $t_G$ , 12 min or more, the  $k^*/(2+k^*)$  term tends to 1.0 at lower flow rates. At a very long  $t_G$  (e.g., 30 min), the increase in the  $k^*/(2+k^*)$  value with flow rate is insignificant beyond 0.5 mL/min. A comparison of Fig. 6A, where  $\Delta\% B = 100$ , and Fig. 6B, where  $\Delta\% B = 40$ , illustrates

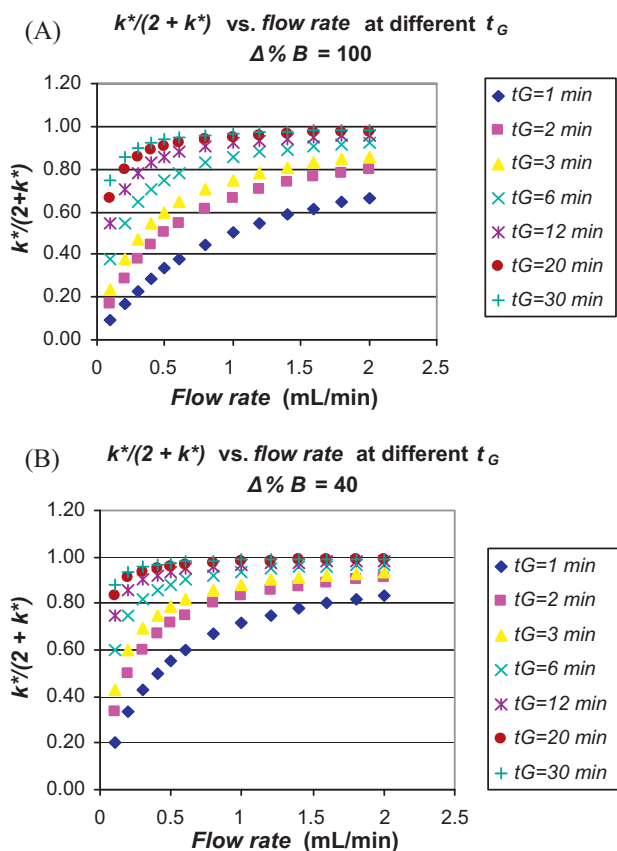


**Fig. 6.** A theoretical plot of the impact of flow rate ( $F$ ) on the retention term ( $k^*$  term) in the  $R_s$  Eq. (7) in gradient elution with different gradient times ( $t_G$ ), e.g., 1–30 min, with two  $\Delta\% B$  values [100 in (A) and 40 in (B)]. Column:  $2 \times 50$  mm.

that flow rate has overall a smaller effect on the  $k^*/(2+k^*)$  term in a shallower gradient, at all values of  $t_G$ .

#### 4.4.2. Comparison of experimental and theoretical resolutions as a function of flow rate

We calculated the theoretical  $R_s$ , using Eq. (7), for the experiments conducted at different flow rates from 0.1 to 1 mL/min, for which the experimentally obtained  $R_s$ , obtained using Eq. (1), was already presented above (Fig. 5). Each calculated term in Eq. (7) –  $N^{1/2}$ ,  $k^*/(2+k^*)$ ,  $\ln(\alpha)$ , and  $R_s$  – at different flow rates is plotted against flow rate in Fig. 7. Column efficiency  $N$  at different flow rates was calculated using  $N = 5.54 (t_R/W_{1/2})^2$  for compounds 2, 4 and 5 from the isocratic elution experiments conducted for this purpose. The  $N^{1/2}$  from compound 5 is used in the plot shown and also for the calculation of the  $R_s$  of the three critical pairs with the assumption that column efficiency is the property of a column, staying the same in either isocratic elution or gradient elution, and that it is analyte independent. It needs to be pointed out that we did not observe the optimum  $N$ , which is presumably at or below 0.1 mL/min, indicating the optimal flow rate to be lower than expected from the Van Deemter curves shown in text books and product brochures. Similar phenomenon was also observed by Jemal and colleagues [18]. The selectivity  $\alpha$  was calculated using equation  $\alpha = k_2/k_1$  in which  $k_1$  and  $k_2$  ( $k = k_g$ , gradient retention factors) were obtained using Eq. (5).

The trend of the plot of the calculated theoretical  $R_s$  versus flow rate, shown in Fig. 7D, for each of three pairs of compounds, matches quite well with the plot of experimental  $R_s$ , obtained using Eq. (5), versus flow rate shown in Fig. 5A. There is a 2-fold difference between the two sets of the  $R_s$  values and this may indicate that the  $R_s$  Eq. (7) may need a correction factor. Nonetheless, we

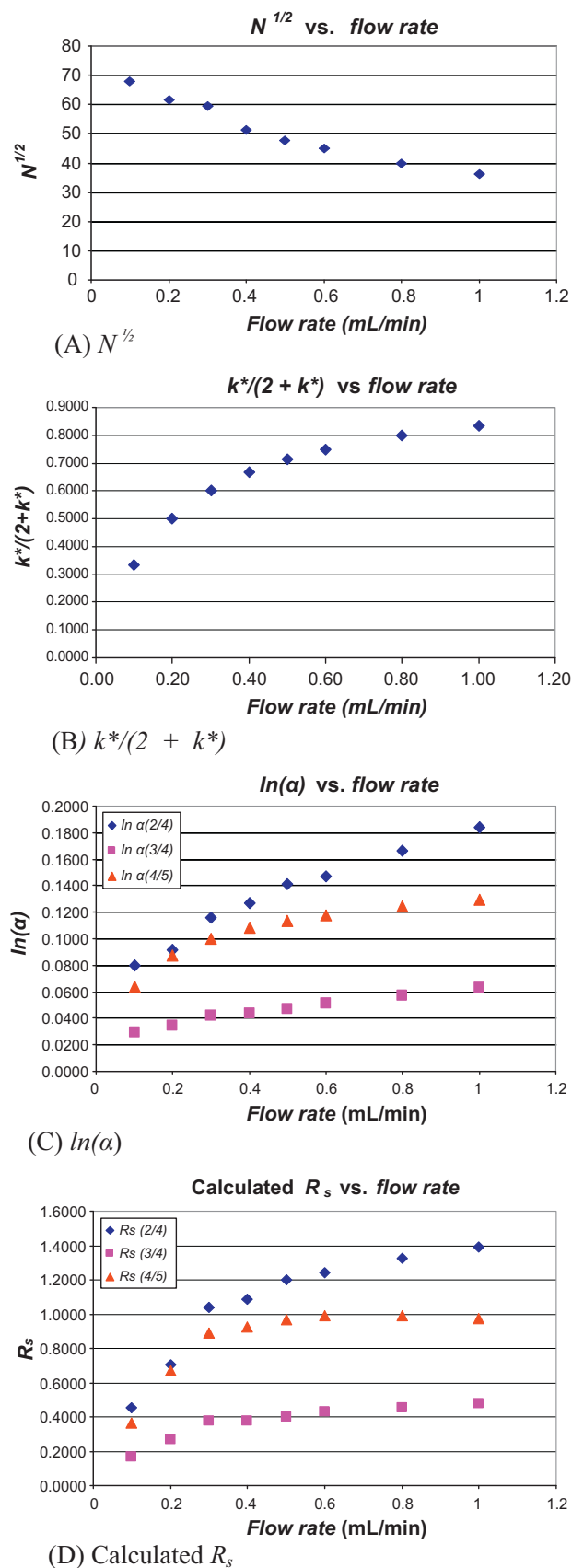


**Fig. 7.** Calculated  $N^{1/2}$ ,  $\ln(\alpha)$ ,  $k^*/(2+k^*)$ , and  $R_s$  vs. flow rate  $F$  on a Luna C18 (2),  $2 \times 50$  mm,  $5 \mu\text{m}$  column.  $N$  values of peak 5 from isocratic elution experiments were used.



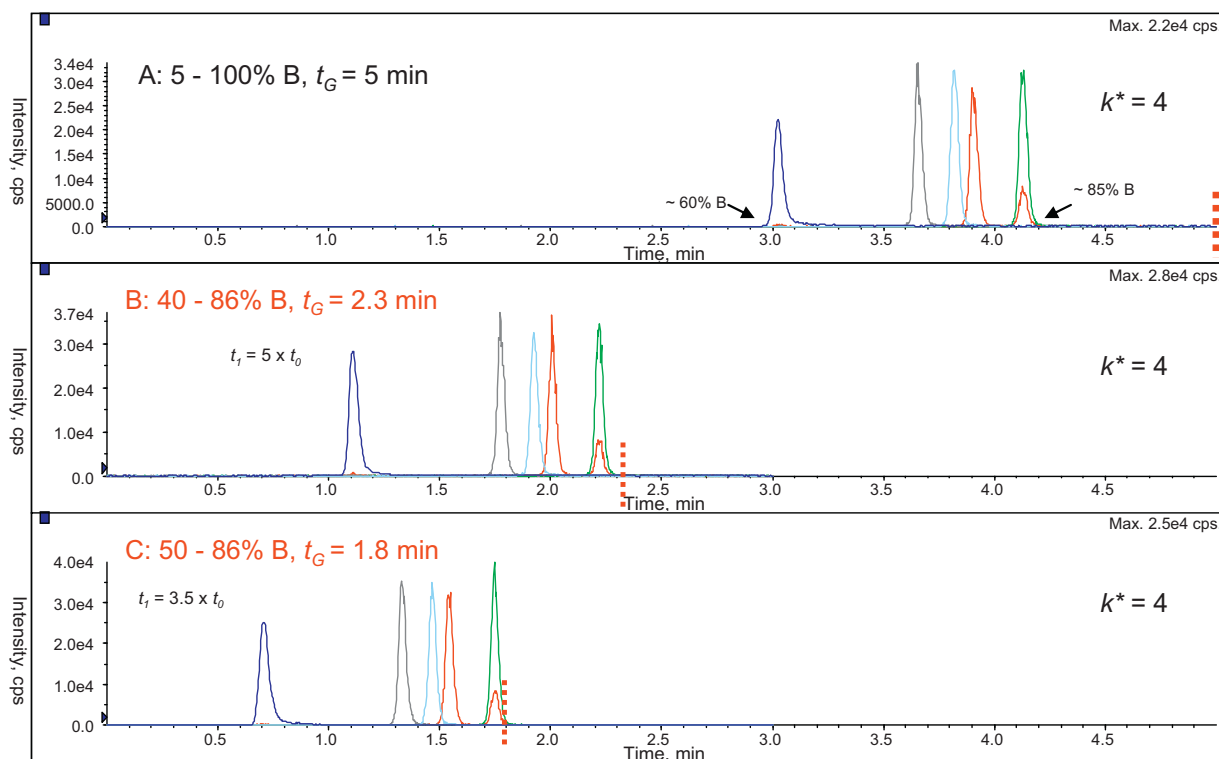


**Fig. 8.** Full range (5–100% B) gradient with  $t_G = 5$  min and  $k^* = 4$  (A). Optimized gradient elution with 40–86% B,  $t_G = 2.3$  min and  $k^* = 4$  (B). Optimized gradient elution with 50–86% B,  $t_G = 1.8$  min and  $k^* = 4$  (C). The column and mobile phases A and B are described in Fig. 1. The dashed vertical line (red) indicates the end of gradient time. (For interpretation of the references to color in this figure legend, the reader is referred to the web version of the article.)

can conclude that we not only theoretically explained why higher resolution can be achieved at higher flow rates but also experimentally confirmed that higher  $R_s$  is achieved at higher flow rates (0.6–1.0 mL/min) in a gradient elution where  $\Delta\% B = 60$  (initial % B = 40 and final % B = 100) and  $t_G = 3$  min.

#### 4.5. Recommended procedures to execute a rapid gradient elution in LC–MS/MS bioanalysis

Adequate resolution and capacity in a gradient elution LC–MS/MS method is required to provide sufficient separation between target analytes which may interfere with each other. It is also important to have enhanced peak capacity/resolution to protect the analytes from unexpected interferences from matrix components. On the other hand, a short run time is always desirable for higher throughput sample analysis.

As shown above, selecting appropriate gradient elution parameters –  $t_G$ , initial and final % B, and flow rate ( $F$ ) – will shorten the run time and improve the resolution and peak capacity on fixed column type and dimensions (stationary phase packing, diameter, length, and particle size) and mobile phases A and B. Column temperature was not included in the current evaluation but rather being fixed. In general, increasing temperature of the column will improve the speed of separation by reducing solvent viscosity and increasing solute diffusion [14,16] as well as increasing peak capacity of the gradient method [17]. A recommended procedure for executing a rapid gradient elution in LC–MS/MS bioanalysis is outlined below.

(1) Select a column, appropriate column temperature (e.g., 40–50 °C), mobile phases A and B which were established during the column and mobile screening phase of method development. Select the highest flow rate that is compatible with the backpressure limit of the LC pump and the acceptable flow rate range for the mass spectrometer. Select a reason-

ably high  $k^*$ , e.g.,  $k^* = 4$ –6 to obtain a value closer to 1.0 for the  $k^*/(2 + k^*)$  term with the goal of balancing between sufficient retention/resolution and gradient time.

- (2) Calculate, using Eq. (6), the  $t_G$  of a full-range gradient elution (e.g., 5–100% B) to achieve the selected  $k^*$  (e.g., 4). Conduct the full-range gradient elution with the calculated  $t_G$  and then examine the resulting chromatogram to determine the retention time  $t_R$  and % B at which the first and last peaks elute. It should be pointed out that this full-range gradient can also be used as the initial gradient in the column and mobile phase screening process.
- (3) Run a few putative shorter gradient elutions by selecting the final % B to be equal to the % B at which the last peak elutes in step 2 and selecting at least two different initial % B values that are 10–30% less than the % B at which the 1st peak elutes in step 2. For each putative elution, a different (shorter)  $t_G$ , calculated using Eq. (6), is used in order to maintain  $k^* = 4$ .
- (4) Examine the resulting chromatograms and select the gradient elution with an initial % B that sufficiently reduces the “wasted” time before the first peak and at the same time does not cause the elution of the first peak too close to the solvent front. In general, it is recommended that  $t_1/t_0$  be  $\geq 3.0$ .
- (5) Assess matrix effect in the selected gradient elution by conducting post-column infusion of the analyte solution while injecting a blank plasma protein precipitation extract, which contains phospholipids and dosing vehicle (e.g., 0.01% PEG400, when applicable).

For demonstration purpose the execution of a gradient elution with the mixture of five compounds shown in Fig. 1 was illustrated in Fig. 8. In this particular example, a flow rate of 0.4 mL/min was selected, the  $t_G$  of a full-range gradient elution (5–100% B) to achieve the selected  $k^* = 4$  was 5 min (Fig. 8A). Two resulting shorter gradients following the suggested procedures are shown in Fig. 8B

and C. The resulting gradient,  $\Delta\% B = 50\text{--}86\%$  with  $t_G = 1.8$  min (Fig. 8C), was chosen as the final gradient when no matrix effect with this method was confirmed. A 3-fold reduction of gradient time  $t_G$  compared to the starting “generic” gradient elution method (Fig. 8A) was achieved while the desired effective retention factor ( $k^* = 4$ ) was maintained. At higher flow rates, e.g., 0.8 or 1.0 mL/min, further reduction in run time (e.g.,  $t_G < 1$  min) and enhancement in resolution were achieved.

## 5. Conclusions

We suggested a systematic and efficient strategy for achieving maximum resolution and speed in rapid gradient LC–MS/S bio-analytical methods. This was based on the fact that the gradient time  $t_G$ , the initial and final percentages of the organic component of the mobile phase can be optimized to shorten the run time of a gradient method. It was also demonstrated experimentally and explained mathematically using the linear-solvent-strength (LSS) gradient theory that increasing flow rate improves both resolution and peak capacity in a rapid gradient method, even with a  $5\ \mu\text{m}$  particle column. This derives from the fact that, in gradient mode, any decrease in column efficiency at higher flow rate is more than compensated by the corresponding increase in  $k^*$ . This effect is less pronounced for longer gradient, where the  $k^*/(2+k^*)$  term of the resolution equation reaches a plateau at lower flow rates. This suggests that speed and high resolution analysis are achieved simultaneously at higher flow rates in rapid bioanalytical gradient elution contrary to the conventional wisdom that a compromise must be made between resolution and speed. Taking this further, there is even more advantage to use high flow rates with sub- $2\ \mu\text{m}$  columns in rapid gradient elution not only because of the slower decrease or flattening in  $N$  with increase of flow rate, which has been broadly discussed in the literature [19–22], but also because

of the increase in the retention  $k^*$  term ( $k^*/(2+k^*)$ ) at higher flow rates.

## Acknowledgement

We would like to thank Dr. Yingru Zhang at Bristol-Myers Squibb for valuable discussion on chromatographic theory.

## References

- [1] L. Romanyshyn, P.R. Tiller, C.E. Hop, *Rapid Commun. Mass Spectrom.* 14 (2000) 1662.
- [2] Y.F. Cheng, Z. Lu, U.D.U. Neue, *Rapid Commun. Mass Spectrom.* 15 (2001) 141.
- [3] P.R. Tiller, L. Romanyshyn, L.U.D. Neue, *Anal. Bioanal. Chem.* 377 (2003) 788.
- [4] K.W. Dunn-Meynell, S. Wainhaus, W.A. Korfmacher, *Rapid Commun. Mass Spectrom.* 19 (2005) 2905.
- [5] J. Mohammed, Y.Q. Xia, *Curr. Drug Metab.* 7 (2006) 491.
- [6] Y. Hsieh, W.A. Korfmacher, *Curr. Drug Metab.* 7 (2006) 479.
- [7] R.N. Xu, L. Fan, M.J. Rieser, T.A. EL-Shourbagy, *J. Pharm. Biomed. Anal.* 44 (2007) 342.
- [8] W.Z. Shou, J. Zhang, *Expert Opin. Drug Metab. Toxicol.* 6 (2010) 321.
- [9] L.R. Snyder, J.W. Dolan, J.R. Gant, *J. Chromatogr.* 165 (1979) 3.
- [10] L.R. Snyder, J.J. Kirkland, J.L. Glajch, *Practical HPLC Method Development*, 2nd ed., John Wiley & Sons, Inc., 1997.
- [11] L.R. Snyder, J.W. Dolan, *High-Performance Gradient Elution*, John Wiley & Sons, Inc., 2007.
- [12] U.D. Neue, J.L. Carmody, Y.F. Cheng, Z. Lu, C.H. Phoebe, T.E. Wheat, *Adv. Chromatogr.* 41 (2001) 93.
- [13] U.D. Neue, *J. Chromatogr. A* 1079 (2005) 153.
- [14] U.D. Neue, J.R. Mazzeo, *J. Sep. Sci.* 24 (2001) 921.
- [15] U.D. Neue, *J. Chromatogr. A* 1184 (2008) 109.
- [16] X. Wang, D.R. Stoll, A.P. Schellinger, P.W. Carr, *Anal. Chem.* 78 (2006) 3406.
- [17] P. Petersson, A. Frank, J. Heaton, M.R. Euerby, *J. Sep. Sci.* 31 (2008) 2346.
- [18] M. Jemal, Z. Ouyang, Y.Q. Xia, *Biomed. Chromatogr.* 24 (2010) 2.
- [19] J.R. Mazzeo, N.D. Neue, M. Kele, R.S. Plumb, *Anal. Chem.* 77 (2005) 460A.
- [20] S. Wainhaus, C. Nardo, R. Anstatt, S. Wang, K. Dunn-Meynell, W. Korfmacher, *Am. Pharm. Rev.* 13 (2010) 40.
- [21] S. Fekete, K. Ganzler, J.J. Fekete, *J. Pharm. Biomed. Anal.* 51 (2010) 56.
- [22] K.J. Fountain, U.D. Neue, E.S. Grumbach, D.M. Diehl, *J. Chromatogr. A* 1216 (2009) 5979.